R10

Time-Domain Correlation Image Sensor: First CMOS Realization of Demodulator Pixels Array

Shigeru ANDO and Akira KIMACHI
Dept. Mathematical Engineering and Information Physics, University of Tokyo
7-3-1 Hongo, Bunkyo-ku, Tokyo 113-8656, JAPAN
Phone: +81-3-5841-6925, Fax: +81-3-5841-8596
E-mail: ando@alab.t.u-tokyo.ac.jp

Introduction

In CCD/AIS Workshop'97, Bruges, we have proposed the basic concept of time-domain correlation image sensor[1] which enables us to detect high frequency modulated light without increasing the scanning rate of image sensor. We also emphasized the importance of temporal correlation in image measurement and analysis by presenting possible applications and simulation results of the correlation image sensor[2]. We realized an 8×8 sensor in discrete components [3] and took several attempts for optimal cell structures [4]. In this paper, we report the successful fabrication results of 16×16 and 64×64 correlation image sensors using a CMOS process available at VDEC at the University of Tokyo, Japan. We describe in detail the layout design of the pixel circuit and evaluate the fabricated sensors through experiments.

Time-Domain Correlation Image Sensor

The time-domain correlation image sensor is an array of correlation demodulators of incident light. It is characterized by: 1) photodetectors that convert light intensities $f_{ij}(t)$ into photocurrents; 2) a reference signal $g(t)$ that is fed commonly to all pixels; 3) current-mode multipliers that generate the product of $f_{ij}(t)$ and $g(t)$; 4) capacitors that integrate the product $f_{ij}(t)g(t)$ and store the results as charges; and 5) CCD or MOS switches for readout of the correlation results [1, 2]. Figure 1 shows why the tight coupling of pixel and correlator is essential for removing "scanning bottleneck" of the correlation operation. The output of this sensor at pixel (i, j) is thus

$$\phi_{ij}(t) = \int_{t-T}^{t} f_{ij}(\tau) g(\tau) d\tau \qquad (1)$$

where T is the integration time.

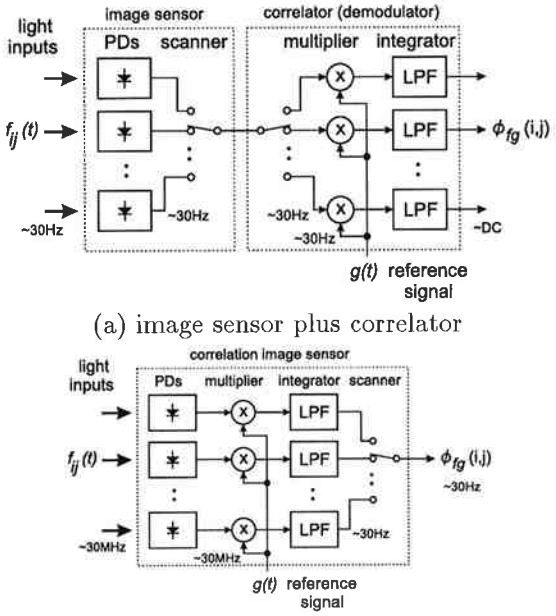

(a) image sensor plus correlator

(b) correlation image sensor

Figure 1: Comparison of time-domain correlation using conventional image sensor and correlation image sensor. The "scanning bottleneck" is thoroughly removed, and the frequency limit of the light modulation and the reference signal can be extended to the limit of PD and multiplier.

Principle of Operation

The pixel circuit we realized is based on a variable transconductance multiplier with capacitive loads [1, 2] (Figure 2). The photocurrent $I_{PD}(t)$ generated by the photodiode PD are divided into drain currents $I_{D+}(t)$ and $I_{D-}(t)$ of the PMOS pair M_1 and M_2,

respectively, with

$$I_{D\pm}(t) = \frac{I_{PD}(t)}{2} \pm g_m(t)\frac{\Delta V_{MPY}(t)}{2}, \quad (2)$$

where $g_m(t)$ and $\Delta V_{MPY}(t) = V_{MPY-}(t) - V_{MPY+}(t)$ are the transconductance and differential gate voltage between M_1 and M_2, respectively. With M_1 and M_2 in the subthreshold region,

$$g_m(t) = \rho I_{PD}(t) \quad (3)$$

where ρ is a constant. Therefore, denoting the charge accumulated at the capacitors C_1, C_2 over a frame T by $Q_\pm(t) = \int_{t-T}^{t} I_{D\pm}(\tau)d\tau$, we find

$$Q_+(t) - Q_-(t) = \rho \int_{t-T}^{t} I_{PD}(\tau)\Delta V_{MPY}(\tau)d\tau \quad (4)$$

$$Q_+(t) + Q_-(t) = \int_{t-T}^{t} I_{PD}(\tau)d\tau, \quad (5)$$

that is, the charge difference $Q_+(t) - Q_-(t)$ gives temporal correlation (correlation output) between $I_{PD}(t)$ and $\Delta V_{MPY}(t)$ whereas the total charge $Q_+(t) + Q_-(t)$ gives the average intensity (intensity output) of the incident light. The charges $Q_\pm(t)$ are read out through the NMOS switches M_3 and M_4.

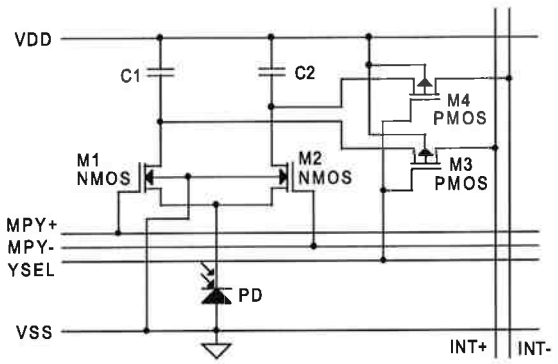

Figure 2: Pixel circuit based on a transconductance multiplier/integrator and MOS readout circuit.

Extended Common-Source/Drain Layout

We designed the layouts of the pixel circuit in Figure 2. For reducing pixel size, we designed PD, M_1, M_2, C_1, and C_2 as a single MOS transistor by extending the common source and the drains of the differential MOS pair M_1, M_2 to use them as the photodiode PD and capacitors C_1, C_2, respectively (Figure 3–??). C_1 and C_2 consist of 1) capacitance between the drain diffusion and metal 1, and 2) junction capacitance between the drain diffusion and the substrate.

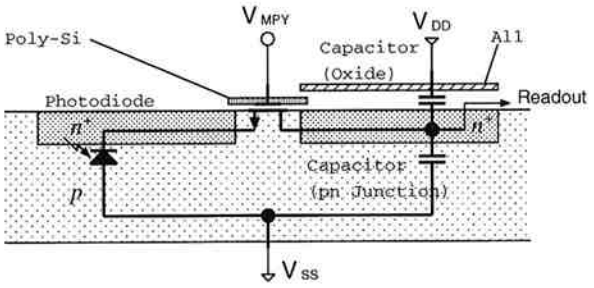

Figure 3: Schematic cross section of the pixel with the extended common-source/drain structure.

Table 1: Fabricated chips and processes.

	MOT97	NEL98	MOT98
chip size	2.3×2.3mm	2.3×2.3mm	7.3×7.3mm
pixel size	75×75μm	60×60μm	60×60μm
image size	8×8	16×16	64×64
process	1.2μm,n-well	0.5μm,n-well	1.2μm,n-well
	2-poly, 2-Al	1-poly, 2-Al	2-poly, 2-Al
mpy/sw Tr	N/P MOS	P/N MOS	P/N MOS
scanning	none	MOS	MOS

Chip Fabrication

We fabricated this layout three times using CMOS processes provided by NTT Electronics (0.5μm) and Motorola Japan (1.2μm) as listed in Table 1. The designs differ each other in
1) pixel size, image size, area ratio of PD and capacitor,
2) choice of NMOS and PMOS for M_1, M_2 for better performance of PD, M_1, M_2, C_1, and C_2, and
3) power distribution, isolation, and light shielding for minimizing symmetry error, substrate resistance, photocarrier leakage, etc.

In the NEL97 chip shown in Table 1, a sensor array of 16×16 pixels, each 60μm×60μm in size, was fabricated along with X and Y address decoders and an output multiplexer (Figure 4). In 7.3mm×7.3mm MOT98 chip, the array size was increased to 64×64 pixels (Figure 5).

Chip Evaluation

We have made several experiments with the 64×64-pixel sensor of the MOT98 chip. Figure 6 plots the correlation output for LED illumination and ΔV_{MPY} both modulated at 1kHz, against their phase difference ϕ. The correlation output varies as $\cos\phi$ according to the phase difference. In Figure 7, the cor-

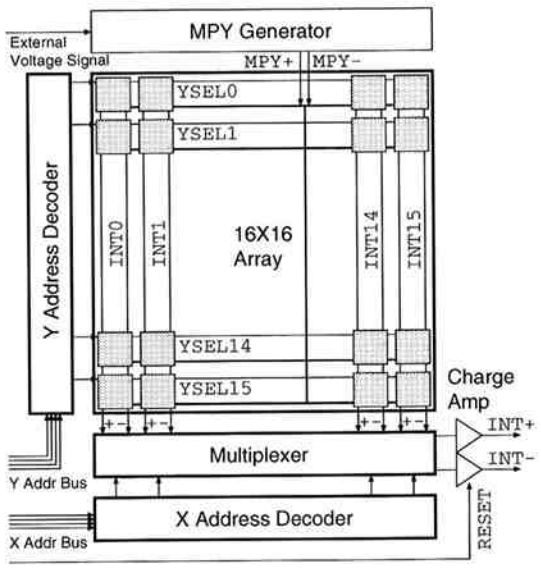

Figure 4: Schematic diagram of the NEL97 16×16 chip. The components with thicker outlines were integrated.

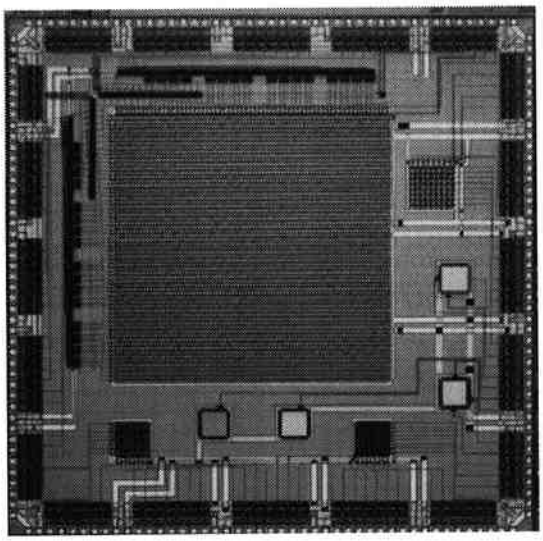

Figure 5: Photograph of the MOT98 chip. The largest block features the 64×64 sensor array.

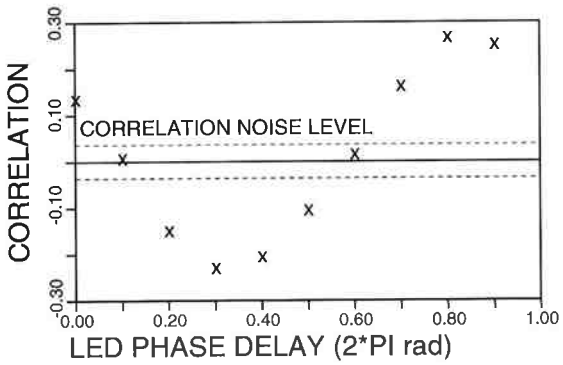

Figure 6: Normalized differential-mode output of the 64×64-pixel sensor the MOT98 chip for 1kHz-modulated illumination and ΔV_{MPY}, plotted against their phase difference ϕ (A_{MPY} = 100mV).

relation output increases in proportion to the amplitude A_{MPY} of ΔV_{MPY} for $A_{MPY} < 50\text{mV} \simeq 2kT/q$ (k: Boltzmann constant) at room temperature ($T \sim$ 300K).

Figure 8 shows the output of MOT98 64×64 sensor array when an "O" pattern was projected by an LED modulated at 1kHz. The correlation output ($\propto \cos\phi$) changes from positive to negative as ϕ increases, while the intensity output does not vary with a phase delay ϕ of the reference signal $\Delta V_{MPY}(t)$.

Compensation of FPN on correlation

The correlation outputs involve fixed pattern noise (FPN) due to the mismatch of MOS differential pair. But we can show that FPN is in proportion to the intensity output, hence can be reduced by priorly estimating the coefficient for each pixel and subtracting from the correlation output.

Application Examples

Although the current devices do not have enough performance, we could demonstrate several applications of the correlation image sensor. Figure 9 show a photograph of the correlation camera in which a MOT98 chip (64×64 pixels), timing logics, reference signal drivers, and video amplifiers are assembled.

Figure 10 illustrates a method for an application to the lock-in photometry. The correlation output is the contribution of the modulated light only in spite of any disturbing illumination. Figure 11 shows the results taken by the correlation camera. The SNR of the correlation output was about 12dB.

References

[1] S. Ando *et al.*, in *Proc. IEEE Workshop on CCD and Advanced Image Sensors*, Bruges, Belgium, 1997.

[2] S. Ando *et al.*, in *Proc. Transducers '97*, vol. 1, pp.307-310, Chicago, IL, USA, 1997.

[3] T. Sakaguchi *et al.*, in *Tech. Digest of 15th Sensor Symp.*, pp.111-114, Kawasaki, Japan, 1997.

[4] A. Kimachi *et al.*, *J. IEEJ*, vol. **E-119**, no. 1, 1999 (submitted; in Japanese).

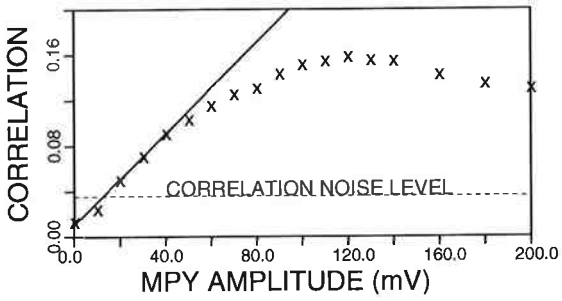

Figure 7: Normalized differential-mode output for 1kHz-modulated illumination and ΔV_{MPY} with $\phi = 0$, plotted against A_{MPY}, the amplitude of ΔV_{MPY}.

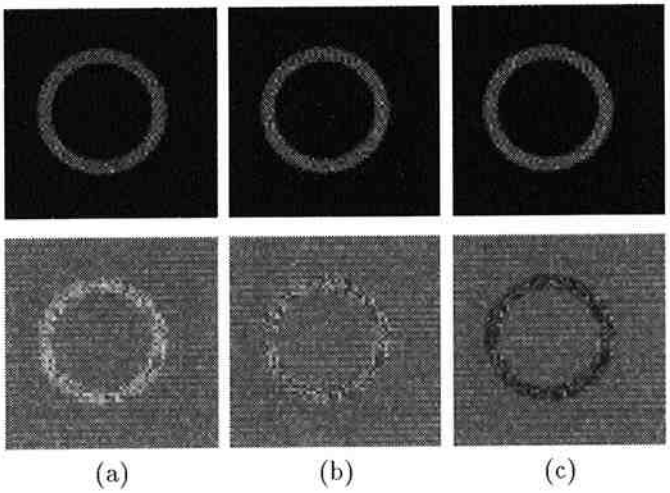

Figure 8: Output of MOT98 chip for an "O" pattern projected by an LED light under 1kHz modulation. The reference signal $\Delta V_{MPY}(t)$ was given with phase delay ϕ. Top: intensity output $Q_+ + Q_-$. Bottom: correlation output $Q_+ - Q_-$. (a) $\phi = 0°$. (b) $\phi = 90°$. (c) $\phi = 180°$.

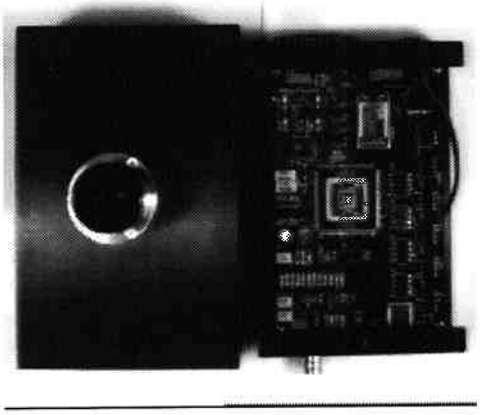

Figure 9: A photograph of the correlation camera (left) and its circuit board (right) in which a 64×64 correlation image sensor is installed with a timing logic, reference signal drivers, and video amplifiers.

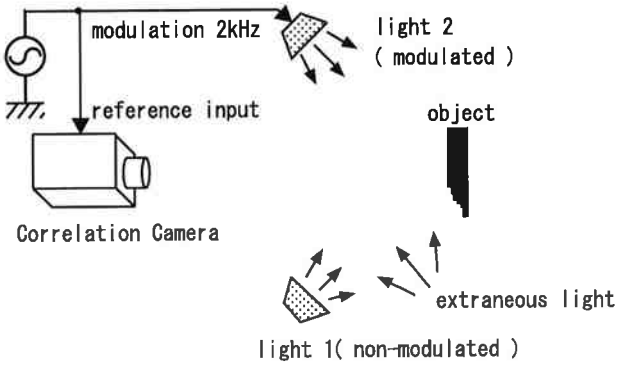

Figure 10: An experimental setup for the separation of modulated illumination for the lock-in photometry, stereo ranging, etc.

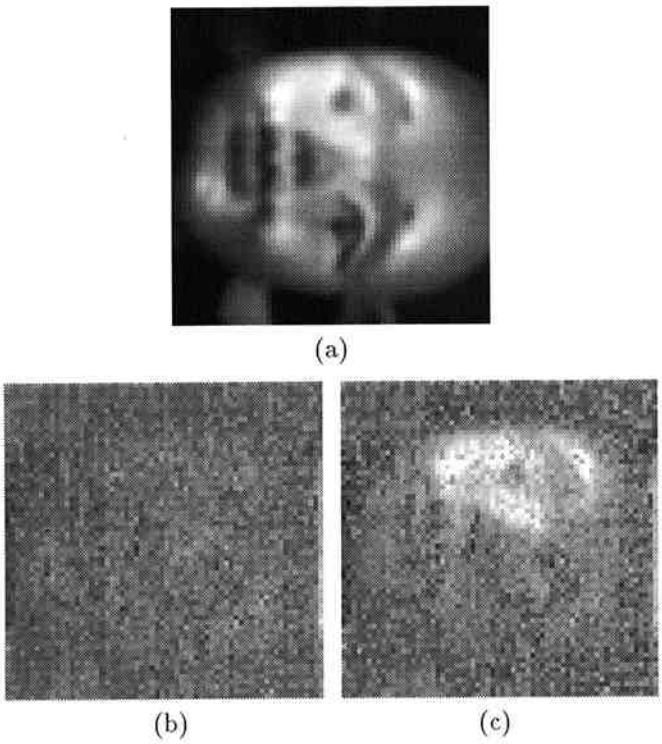

Figure 11: Output of the 64×64 correlation camera for a plaster figure illuminated both by a stationary light and an LED lamp under 2kHz modulation. (a): intensity output. (b) and (c): correlation outputs when the modulation is off and on, respectively. Only the illuminated side of the plaster figure by the modulated light is extracted in (c).